

24. Spectral Features of Foreshocks.

By Masaru TSUJIURA,

Earthquake Research Institute.

(Received Sept. 30, 1977.)

Abstract

In order to obtain the spectral features of foreshocks in comparison with other events, the spectrum of body waves for three moderate-sized earthquake sequences ($M \geq 5.4$) which were preceded by a considerable number of foreshocks are studied in terms of source parameters. The results obtained here show that the spectrum of the main foreshock is somewhat different from the other events in each region although the relation is not simple. The stress drop of the main foreshock is lower by a factor of about 1/5 than the main shock and major aftershocks (eastern part of Yamanashi pref., 1976) or aftershocks (Kawazu, Izu peninsula, 1976), while the foreshock of Hawaii (1975) shows a relatively higher stress drop compared with the main shock and the shocks in normal activity.

1. Introduction

The relative decrease of high frequency amplitudes for both P and S waves is found in small earthquakes preceding a large shock (FEDOTOV *et al.*, 1972). In this connection, they proposed a possibility to utilize the spectral features of seismic waves for earthquake prediction. WATANABE (1974) suggested that the temporal variation of seismic waveforms is found at the beginning of aftershock sequences, and discussed it in terms of the locality of events including the effects of crushing strength and residual stress. SUYEHIRO (1968) studied the spectrum of seismic waves before and after the Matsushiro earthquake swarm, and suggested that less high frequency components are found for the events after the earthquake swarm. Less high frequency amplitudes of S waves are also found at the beginning of aftershocks than in later events. Fig. 1 shows an example of such aftershocks for the Izu-Hanto-Oki earthquake of 1974. Recently, CHOUET (1976) found the temporal variation of the apparent Q derived from high frequency coda waves of local earthquakes, and discussed it in terms of the temporal variation in the medium properties related to the tectonic stress. Possible time variation of seismic spectra will contribute to a better understanding of tectonic processes in the specific regions.

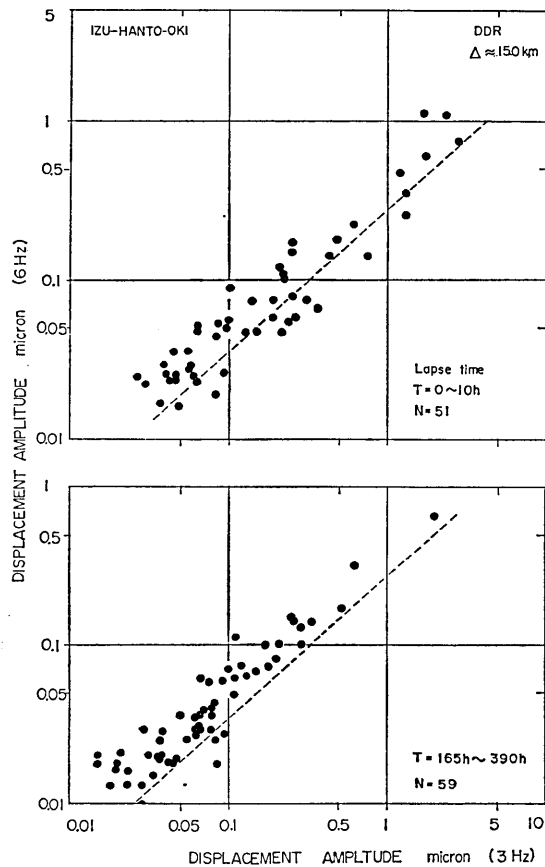


Fig. 1. Relation between the amplitudes of *S* waves at 6 Hz and 3 Hz for the aftershocks of the Izu-Hanto-Oki earthquake of 1974 during the two periods observed at DDR. Small amplitudes of 6 Hz compared with 3 Hz can be seen on the upper figure which obtained for the events at the beginning of the aftershocks (0-10 hours). T; Lapse time measured from the origin time of the main shock.

Since 1972, the observation of the seismic spectrum has been continued by the analog-filtering instrument. No clear evidences indicating the temporal variation of the seismic spectrum have been found. However, some differences in the spectral features are detected in the sequence of the foreshocks, the main shock and the aftershocks. MOGI (1967, 1968) pointed out that some of the major earthquakes were preceded by a considerable number of foreshocks, which were concentrated in the main shock area. If the foreshocks can be discriminated from the other shocks in their spectral features, a continuous monitoring of the

spectral variations of seismic waves will give us some information useful for earthquake prediction.

2. Data

We observed recently three moderate-sized earthquakes which were preceded by a number of foreshocks. The earthquake parameters of the main shocks are shown in Table 1 together with the parameters of the

Table 1. List of the event parameters of the main shock and its largest foreshock.

Date	Time h m s	Epicenter	Depth km	m_b	M_s, M	Region
75 Nov. 29	13 35 40.5	19°36' N 155°05' W	8.0	5.8	5.1	Hawaii*
75 Nov. 29	14 47 40.4	19 33 N 155 02 W	5.0	6.0	7.1	Hawaii*
76 June 16	05 34 01.6	35 31 N 139 00 E	20		4.7	Yamanashi**
76 June 16	07 36 19.9	35 30 N 139 00 E	20		5.5	Yamanashi**
76 Aug. 18	00 55 11.6	34 46 N 138 58 E	2.8		2.9	Kawazu, Izu***
76 Aug. 18	02 18 59.7	34 47 N 138 57 E	0		5.4	Kawazu, Izu**

*: Event parameters determined by USGS.

** : determined by JMA.

***: determined by TSUMURA *et al.* (1977).

largest foreshocks which occurred within a few hours before the main shocks. In order to obtain the spectral feature of the foreshocks in comparison with the other events, the spectrum of body waves are studied for each earthquake sequence.

Fig. 2 shows the location of seismic stations. All signals are telemetered by the radio waves to the Earthquake Research Institute (ERI), and recorded on ink-writing chart recorders and on magnetic tape. Moreover, three sets of the identical analog-type spectrum analyzers connected to the short-period seismograph are operated continuously in order to obtain the spectrum of local earthquakes (TSUJIURA, 1966, 1967, 1969). The data used in this study are given mainly by short-period spectrum analyzers. The data of long-period (LP), medium-period (MP), wide-band (WB) and ultra long-period (ULP) seismographs (TSUJIURA, 1965, 1973) are also used for larger events ($M > 3.5$) using the analog-type band-pass filters (TSUJIURA, 1973).

3. Result

The largest foreshock ($M=4.7$) occurred about 2 hours before the main shock ($M=5.5$) in eastern part of Yamanashi prefecture, and a considera-

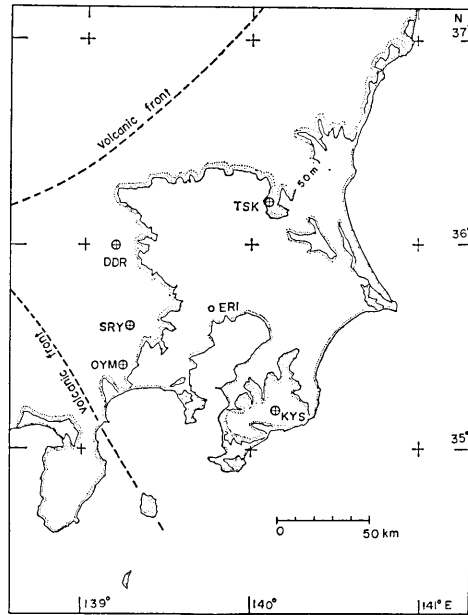


Fig. 2. The seismic telemetering network in the Kanto district.

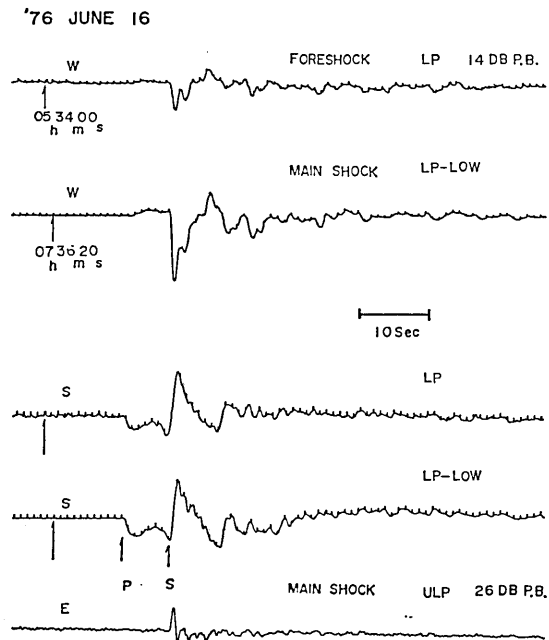


Fig. 3. Comparison of the seismograms of the foreshock and the main shock recorded on long-period (LP, LP-Low) seismographs at DDR. LP-Low means that the magnification of LP-Low is a factor of 1/10 for LP. Impulsive forms on the LP seismograms indicate second marks.

ble number of shocks followed this foreshock (UCHIKE and ICHIKAWA, 1976). Fig. 3 shows the comparison of seismograms for the largest foreshock and main shock recorded on LP, LP-Low and ULP seismographs at DDR which located at about 50 km from the epicenter of the main shock. LP-Low means the low magnification at a factor of 1/10 for LP. These seismograms show similar waveforms, although their absolute amplitudes differ by more than a factor of 10. A similarity in waveform for both events suggests that they have similar source mechanisms (HAMAGUCHI and HASEGAWA, 1975). In fact, the distribution of *P*-wave first motion data is almost the same except at few stations including Fujigawa (138°25'E, 35°13'N) and Inuyama (137°03'E, 35°35'N), which lie near the nodal lines. Fig. 4 shows a comparison of seismograms for foreshock and major aftershocks recorded on the medium-period seismograph (MP) at DDR. Although the amplitudes of high frequencies between *P* and *S* waves are almost the same, within a factor of 2, the relatively longer-period of the *P*-wave first motion can be seen directly on the seismogram of the foreshock. Fig. 5 shows the filtered seismograms through the band-pass filters with one octave bandwidth. Less high frequency amplitudes of the

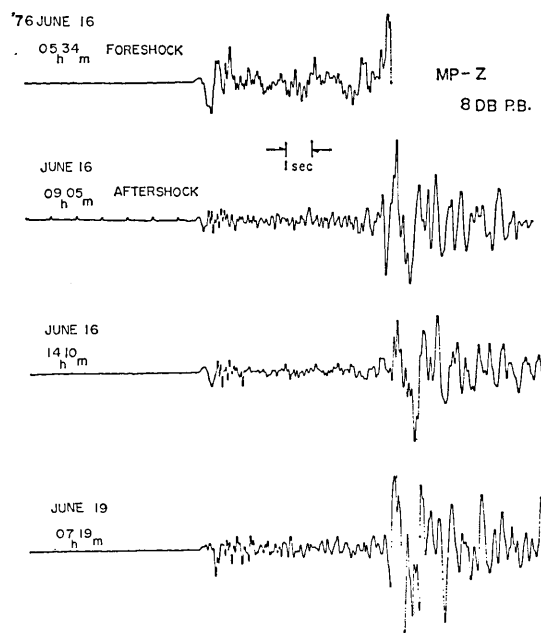


Fig. 4. Comparison of the seismograms for the foreshock and major aftershocks recorded on the medium-period (MP) seismograph at DDR. Note the low-frequency *P* waves of the foreshock compared with the aftershocks.

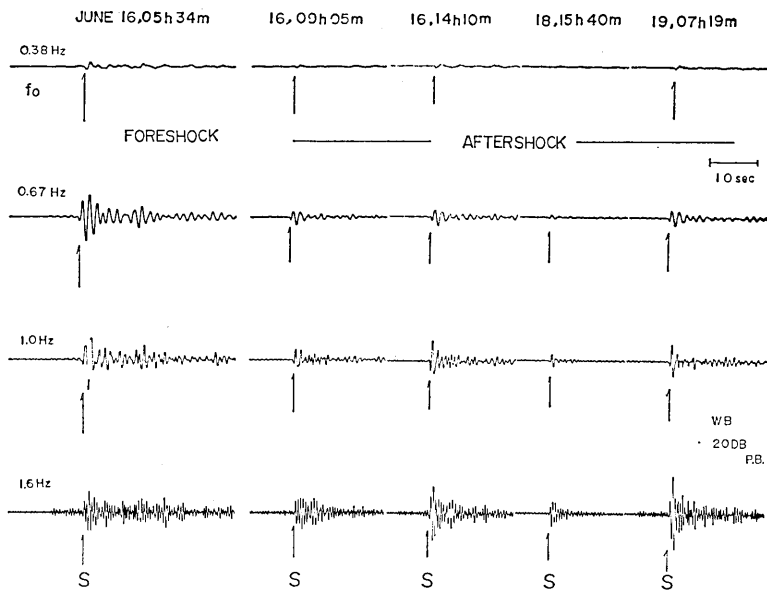


Fig. 5. An example of the filtered seismograms. f_0 indicates the center frequency of the band-pass filter with one octave bandwidth. Note less high-frequency amplitudes (1.6 Hz) at the main arrival of the foreshock, but distributed over a longer time.

foreshock, but distributed over longer time are also shown on the seismograms of S waves. Based on these records, and by the use of the band-pass filters with $1/3$ octave bandwidth the spectrum of the S waves is studied.

Following AKI and CHOUET (1975), the Fourier transform $F(\omega)$ of displacement due to far field S waves in an unbounded homogeneous elastic medium at a distance r from the source can be written as

$$|F(\omega)| = C(4\pi\rho\beta^3r)^{-1}\dot{M}(\omega)$$

where C is a geometrical factor equal to or less than 1, ρ is the density, β is the shear-wave velocity, and $\dot{M}(\omega)$ is the Fourier transform of the time derivative of seismic moment. For a band-pass signal with $|F(\omega)| = F$ (constant) in $\omega_2 < |\omega| < \omega_1$, $|F(\omega)| = 0$ otherwise, and $\phi(\omega) = 0$ for all ω , the corresponding signal $f(t)$ is written as

$$\begin{aligned} f(t) &= \frac{1}{2\pi} \int_{-\omega_1}^{-\omega_2} F e^{i\omega t} d\omega + \frac{1}{2\pi} \int_{\omega_2}^{\omega_1} F e^{i\omega t} d\omega \\ &= 2Ff_1 \frac{\sin \omega_1 t}{\omega_1 t} - 2Ff_2 \frac{\sin \omega_2 t}{\omega_2 t} \end{aligned}$$

where $f_2 = \omega_2/2\pi$ and $f_1 = \omega_1/2\pi$. The maximum amplitude at $t=0$ is equal to

$$f_0 = 2F(f_1 - f_2) = 2F\Delta f.$$

Thus for a rough approximation the amplitude of a wavelet is the product of its amplitude spectral density and twice the bandwidth. From the known bandwidth of the band-pass filter and the maximum amplitude of the S wave measured on each frequency, the amplitude spectral density $|F(\omega)|$ of S wave is estimated.

Fig. 6 shows the source spectrum of the S wave for five major events obtained by the method described above, and by the correction of attenuation assuming the shear-wave velocity to be 3.5 km/sec and Q_β 400 (TSUJIURA, 1977). Moreover, DDR has a site effect (TSUJIURA, 1977), which may be corrected by dividing the observed spectra by 2.5 for $f < 1.5$ Hz and 1.5 for $f = 3$ Hz. The origin time for each event is shown at the end of the corresponding curve. Since our data consist of the band-pass filter

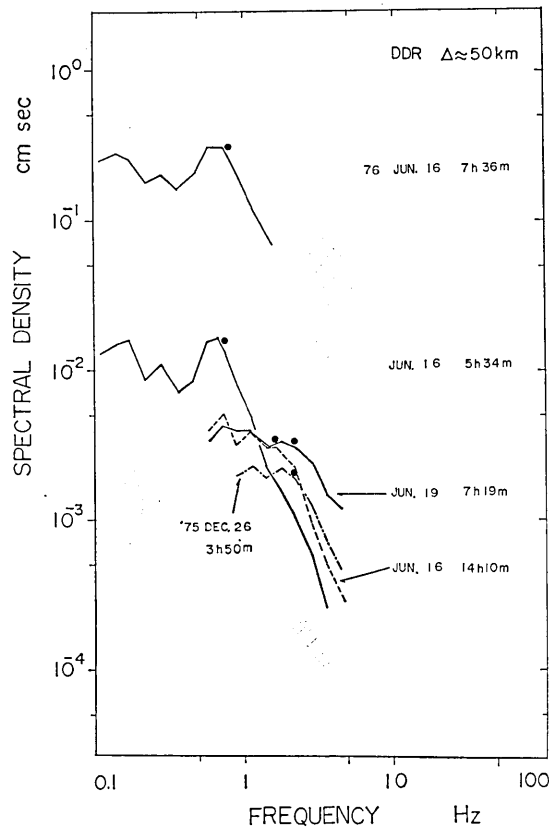


Fig. 6. Source spectrum of S waves for the major events in the earthquake sequence of the eastern part of Yamanashi prefecture.

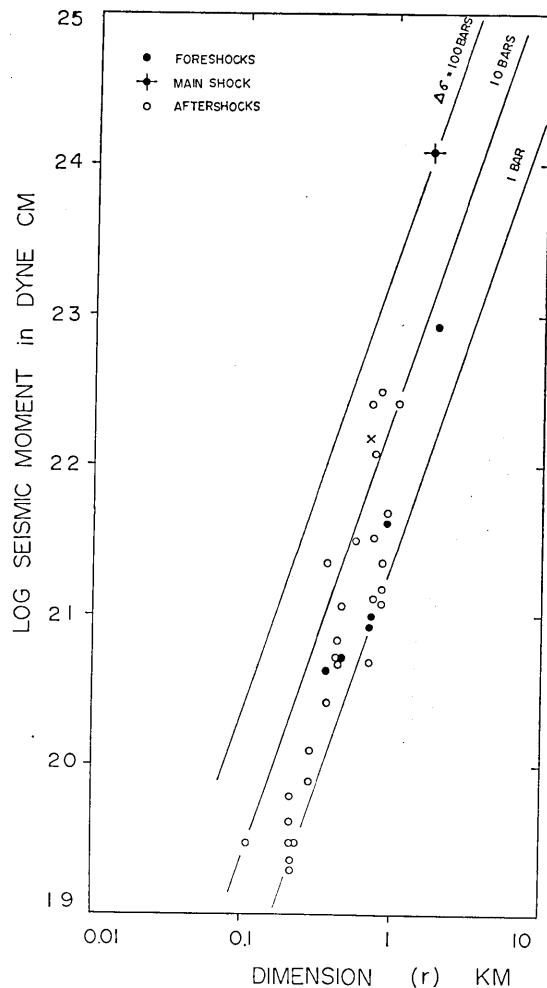


Fig. 7. Relation between the log seismic moment to source radius derived from the corner frequency for the earthquake sequence of the eastern part of Yamanashi prefecture. Diagonal lines show constant stress drops.

records, a constant long-period level (Ω_0), a spectral corner frequency (f_c) and a high frequency spectral asymptote are not determined uniquely, therefore these values are approximated by reducing them to two straight lines that intersect at the corner frequency. The approximated f_c are shown by black dots. It is clearly shown that the corner frequency of the foreshock (June 16, 5h 34 m) is small compared with the other events.

Fig. 7 shows the source parameter of this series obtained from the Brune's formula (BRUNE, 1970), assuming the values of 2.8 g/cm^3 and 0.8 as the constants of density and geometrical spreading, respectively. We

analyzed six events in the foreshock series (closed circles), since the other events are too small to be analyzed accurately. The cross mark represents the source parameter for the largest event of Dec. 26 03h 50 m, 1975, in this area during the two years before the main shock. It can be seen that the largest foreshock has a relatively lower stress drop (7 bars) compared with the main shock (100 bars) and major aftershocks (about 20 bars). But there is no clear difference of the stress drop between the small foreshocks and aftershocks.

The foreshock with low stress drop is also found for the earthquake sequence of Kawazu, Izu peninsula which occurred about 1.5 hours before the main shock. Detailed description of this earthquake sequence will be given by TSUMURA *et al.* (1977). In the early part of this series, our analog-filtering instruments are connected to TSK ($\Delta=195$ km). These data are too small for the analysis of foreshocks and aftershocks. We therefore studied the pulse width of the first *P*-wave motion using the original seismograms of Okuno (OKN) which is one of the temporary stations of southern Kanto.

Fig. 8 shows the relation between the pulse width of the initial *P*-wave motion (first break to first zero crossing) and its magnitude observed at OKN located at about 18 km from the epicenter of the main shock.

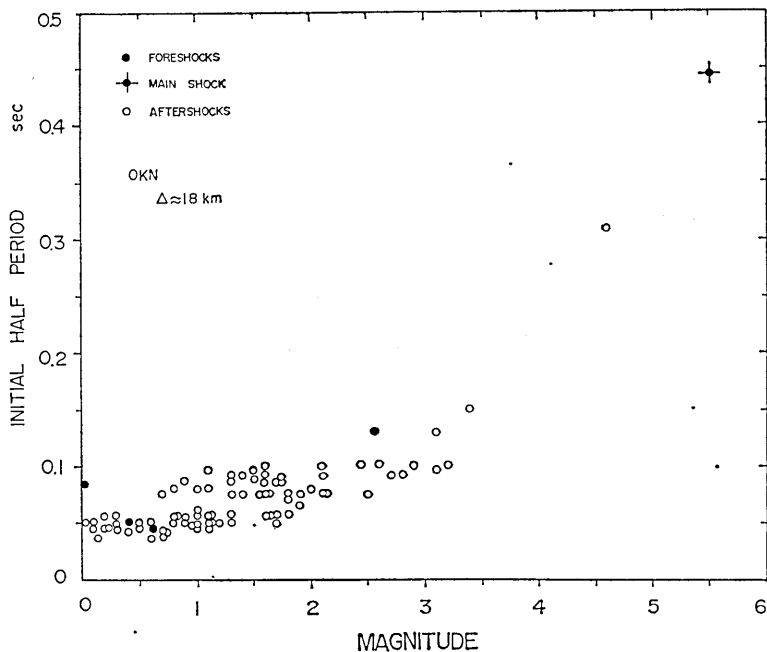


Fig. 8. Relation between the time from first break to first zero crossing in the seismogram of the *P* wave and its magnitude obtained at Okuno (OKN) for Kawazu earthquake.

In this series, magnitudes less than 3.5 are determined by using the formula of Hori (1973) based on the total duration time of the data at DDR. It must be noted that our magnitude is about 0.3 smaller than Tsumura's result.

O'NEILL and HEALY (1973) devised a method to estimate the source radius for small earthquakes from the measurement of the pulse width of the first *P*-wave motion, corrected for Q_α and instrument response. From the source radius and its magnitude, they determined the stress drop. By using the O'Neill and Healy's model assuming a Q_α 200, the source radius of the largest foreshock and two aftershocks with the same magnitude are estimated, and obtained the values of 700, 400 and 200 m, respectively. Using these values and magnitude of 2.9, the stress drops estimated were 0.5 bar for foreshock, and 2 and 8 bars for aftershocks, respectively.

In order to study the spectrum of the *S*-wave for the aftershock sequence, the filtering instrument is connected to OYM located at about 80 km from the epicenter of the main shock. Fig. 9 shows an example of the filtered seismograms. f_0 indicates the center frequency of the band-pass filter with one octave bandwidth. There are some features of the

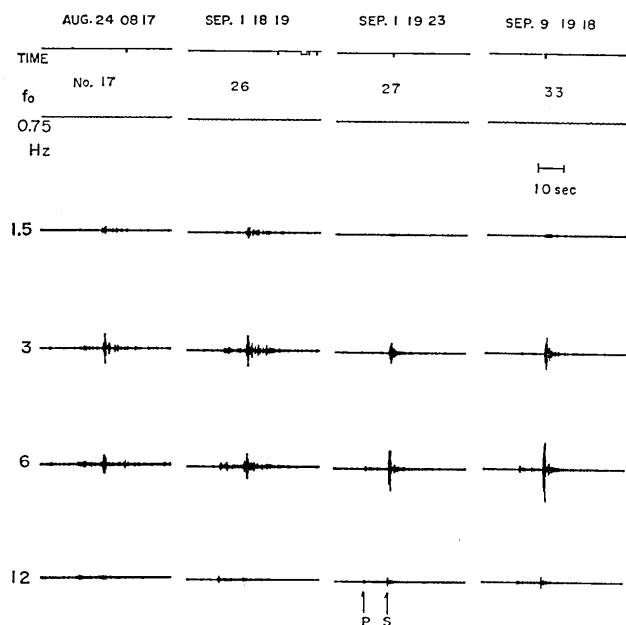


Fig. 9. An example of the filtered seismograms for 4 aftershocks of the Kawazu earthquake. f_0 indicates the center frequency of the band-pass filter with one octave bandwidth. Tick marks at the top are minute marks. Note the differences of the spectra for the events No. 17, 26 and 27, 33.

S-wave spectrum. For example, the two events of the left hand side (event No. 17, 26) contain a relatively larger low frequency component (1.5 Hz) than those of the two events of right hand side (No. 27, 33), while high frequency components (6, 12 Hz) predominate in the two events of the right hand side. The difference of spectrum between events No. 17, 26 and No. 27, 33 corresponds to the difference of roughly two times in the source dimension as will be described later.

Based on these records, we obtained the source spectrum of the *S*-wave, assuming a value of Q_β 300, a shear-wave velocity of 3.5 km/sec and by the correction of the site factor with frequency-dependence (TSUJIURA, 1977), and determined the corner frequency. The value of Q_β used here is somewhat uncertain; we determined a Q_β empirically from the average spectral ratio of *S*-waves based on that of DDR previously determined. From the corner frequency, the source radius a is estimated by using the Madariaga's formula, $a = 0.21 \beta / f_c$ (MADARIAGA, 1976), where β is the shear-wave velocity (3.5 km/sec) and f_c is the corner frequency. Fig. 10 shows the distribution of source radius schematically for the aftershocks generated for about 1 month from 15 hours after the main shock. The difference of the size of circles shows the relative difference of source radius. The maximum and minimum of circles correspond to the source radius of 290 and 90 m, respectively. The source radius obtained here is somewhat small, an average by a factor of 0.7 compared with the values obtained from the O'Neill and Healy's model. The magnitude of these events ranges from 1.5 to 2.5, and there is no systematic difference of the source size corresponding to the magnitude difference. Numerals attached to the circles indicate the event number which corresponds to the events shown in Fig. 9. The locations of the largest foreshock and the main shock are also plotted for the comparison.

The events with relatively large source dimensions are concentrated near the main shock, while the events with small source dimensions are concentrated at the north-west end of the aftershock area, and this tendency appears to be independent of the earthquake magnitude. Although local difference of path effect, especially near the source by the rupture of main shock is to be expected (e.g., SHIBUYA and SUYEHIRO, 1976), the difference of source dimensions must be due to a difference of the static shear strength of the fault zones in this area. Because, as mentioned earlier, the largest foreshock which occurred near the epicenter of the main shock has relatively large source dimensions (700 m), it contrasts with the event with smaller source dimensions (200 m) which occurred at north-west end of the aftershock area. In other words, present result suggests that the event with large source dimensions around the main shock will be due to the result reflected the inherent nature in this area,

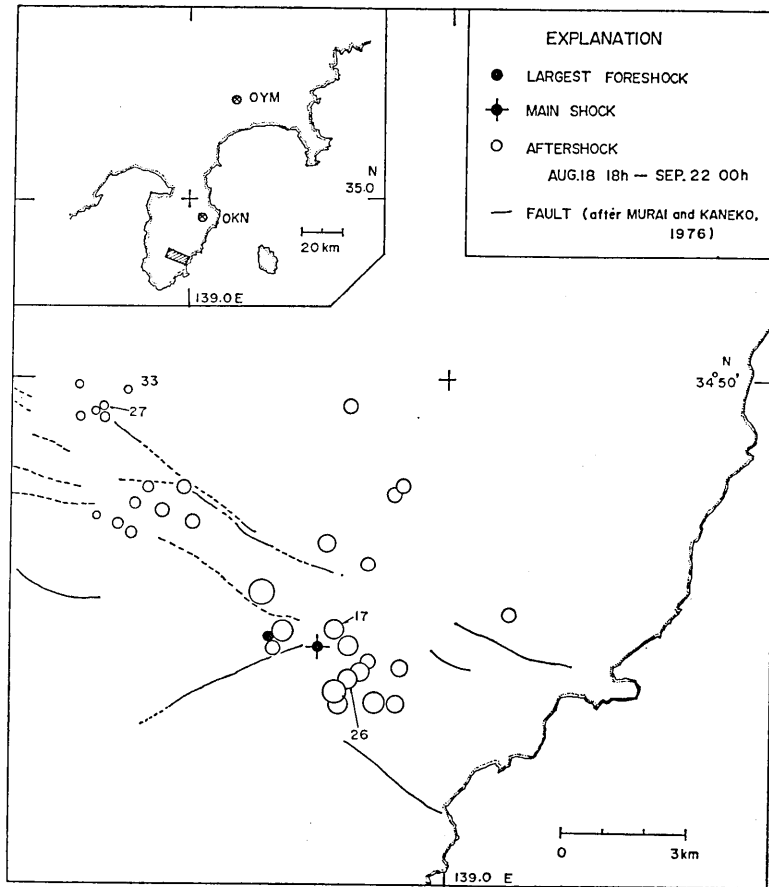


Fig. 10. Map schematically showing the local differences of source size derived from the corner frequency of the *S* waves. Numerals attached to the circles show the event number corresponding to the events of Fig. 9.

rather than the attenuation effect caused by the rupture of the main shock.

On the other hand, the foreshock of Hawaii shows a high stress drop. Fig. 11 shows the original seismograms for the foreshock and the main shock observed by short-period (SP) and long-period (LP, LP-Low) seismographs. A larger short-period amplitude can be seen on the *P*-waves of the foreshock in spite of the fact that the surface-wave magnitude (M_s) is smaller by a magnitude unit of 2.0 than that of main shock. The predominant period for *P* waves of both events are about 1 sec and 10 sec, respectively. The smaller period suggests a relatively higher stress drop. The disagreement of the values of m , determined by USGS and the *P*-wave amplitudes of our short-period seismograms may be in part due to the different characteristics of the seismographs. Our seismograph is

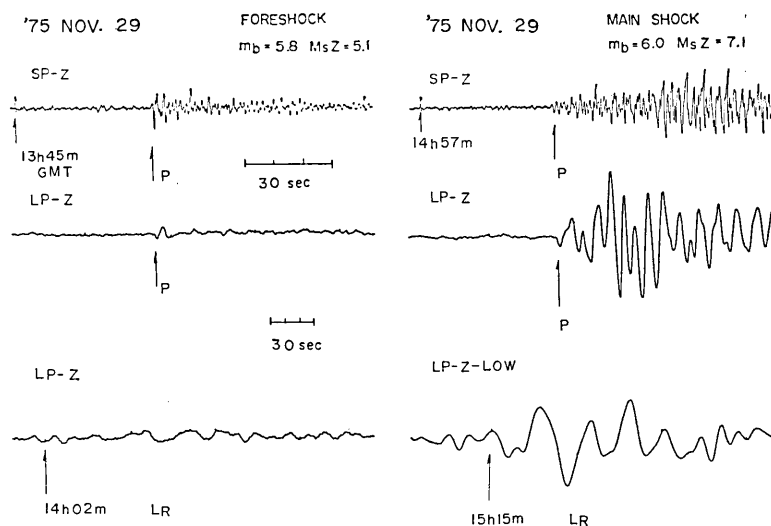


Fig. 11. Comparison of the seismograms of the foreshock and the main shock of the earthquake in Hawaii recorded on short-period (SP) and long-period (LP, LP-Low) seismographs at DDR. Note the different time scale on the SP and LP seismograms.

of the velocity type which has a peak magnification in displacement at 30 Hz, while that of WWSS (standard short-period seismograph) is at about 0.7 Hz. Our seismogram will contain more high frequency waves. Nevertheless, a smaller first motion can be seen on the seismogram of our main shock. This behavior might be attributed partly to the difference in the time function at the source. The main shock of our seismogram suggests the slower source time function, apparently common to the multiple shock as reported by WYSS and BRUNE (1967), or a multiple sequence (TRIFUNAC and BRUNE, 1970). In fact, the maximum amplitude of the *P*-wave group for the main shock appears about 40 sec after the initial motion.

In order to discriminate between the foreshock and the events in the normal seismic activity, however, it is important to know the spectrum of events in the normal activity. In Hawaii (region No. 613, see FLINN and ENGDahl, 1965), the ten earthquakes with magnitude M_L or $m_b > 5.0$ are reported by ISC since 1961. The amplitudes of the *P* waves of the three events with $m_b \geq 5.5$ are examined in their SP and LP seismograms. They show that the relative amplitudes of the *P* waves are the same for that of our main shock. Therefore, at a rough estimation, we may conclude that the foreshock of Hawaii is the event contained the high frequency components which supports the high stress drop. Whatever the case may be, the spectrum of the foreshock seems to be different from those of the other events in each region.

It is hoped that the spectral study of more high frequency waves

from local earthquakes will contribute to discriminating the foreshock more clearly from the normal events, or to find a temporal variation of the seismic wave spectrum as suggested by CHOUET (1976). For this purpose, the analog-filtering instrument with the frequency range up to 200 Hz is installed at TSK.

4. Conclusion

We presented some features of the spectrum of the foreshock. The result shows the differences between the foreshock and the other events, but the relation is not simple. By accumulating similar studies for a wider frequency range in many seismic areas, and studying the geological and seismological setting of their events, we may eventually discuss the possibility of the earthquake prediction based on the seismic spectrum.

Acknowledgment

The writer wishes to express his thanks to Prof. Keiiti Aki who read the manuscript critically and offered many valuable suggestions. The writer also thanks to Dr. Megumi Mizoue for his valuable advice. Gratitude is expressed to Dr. Kenshiro Tsumura and the staff of the expedition team of the Kawazu earthquake for the use of unpublished data of epicenter determination and the seismograms of the Okuno station, and to Dr. Kenichiro Yamashina for providing me with the first motion data of the E. Yamanashi earthquake he collected.

References

- AKI, K., and B. CHOUET, 1975, Origin of coda waves: source, attenuation, and scattering effects, *J. Geophys. Res.*, **80**, 3322-3342.
- BRUNE, J. N., 1970, Tectonic stress and the spectra of seismic shear waves from earthquakes, *J. Geophys. Res.*, **75**, 4997-5009.
- CHOUET, B. A., 1976, Source, scattering and attenuation effects on high frequency seismic waves, preprint.
- FEDOTOV, S. A., A. A. GUSEV, and S. A. BOLDYREV, 1972, Progress of earthquake prediction in Kamchatka, *Tectonophysics*, **14** (3/4), 279-286.
- FLINN, E. A., and E. R. ENGD AHL, 1965, A proposed basis for geographical and seismic regionalization, *Review of Geophysics*, **3**, 123-149.
- HORI, M., 1973, Determination of earthquake magnitude of the local and near earthquake by the Dodaira Micro-earthquake Observatory, *Speci. Bull. Earthq. Res. Inst.*, **10** (4), 1-4, (in Japanese).
- HAMAGUCHI, H., and A. HASEGAWA, 1975, Recurrent occurrence of the earthquake with similar wave forms and its related problems, *Zisin*, II, **28**, No. 2, 153-169, (in Japanese).
- MADARIAGA, R., 1976, The dynamics of an expanding circular fault, *Bull. Seism. Soc. Am.*, **66**, 639-666.
- MOGI, K., 1967, On foreshocks and earthquake swarms, *Zisin*, II, **20**, No. 4, 143-146, (in

- Japanese).
- MOGI, K., 1968, Source locations of elastic shocks in the fracturing process in rocks (1), *Bull. Earthq. Res. Inst.*, **46**, 1103-1125.
- MURAI, I., and S. KANEKO, 1974, The Izu-Hanto-Oki earthquake of 1974 and the earthquake faults, especially, the relationships between the earthquake faults, the active faults, and the fracture systems in the earthquake area, *Speci. Bull. Earthq. Res. Inst.*, **14**, 159-203, (in Japanese).
- O'NEILL, M. E., and J. H. HEALY, 1973, Determination of source parameters of small earthquakes from *P*-wave rise time, *Bull. Seism. Soc. Am.*, **63**, 599-614.
- SHIBUYA, K., and K. SUYEHIRO, 1976, Spectral analysis of the aftershocks of the earthquake off Izu Peninsula, 1974, *J. Phys. Earth*, **24**, 189-203.
- SUYEHIRO, S., 1968, Change in earthquake spectrum before and after the Matushiro swarm, *Pap. Met. Geophys.*, **19**, 427-435.
- TRIFUNAC, M. D., and J. N. BRUNE, 1970, Complexity of energy release during the Imperial Valley, California, earthquake of 1940, *Bull. Seism. Soc. Am.*, **60**, 137-160.
- TSUJIURA, M., 1965, A pen-writing long-period seismograph, part 3, *Bull. Earthq. Res. Inst.*, **43**, 429-440, (in Japanese).
- TSUJIURA, M., 1966, Frequency analysis of seismic waves (1), *Bull. Earthq. Res. Inst.*, **44**, 873-891.
- TSUJIURA, M., 1967, Frequency analysis of seismic waves (2), *Bull. Earthq. Res. Inst.*, **45**, 973-995.
- TSUJIURA, M., 1969, Regional variation of *P* wave spectrum (1), *Bull. Earthq. Res. Inst.*, **47**, 613-633.
- TSUJIURA, M., 1973, Spectrum of seismic waves and its dependence on magnitude (1), *J. Phys. Earth*, **21**, 373-391.
- TSUJIURA, M., 1977, Spectral analysis of the coda waves from local earthquakes, preprint.
- TSUMURA, K., I. KARAKAMA, I. OGINO, K. SAKAI, and M. TAKAHASHI, 1977, Observation of the earthquake swarm in the Izu peninsula (1975-1977), *Bull. Earthq. Res. Inst.*, **52**, 113-140, (in Japanese).
- UCHIIKE, H., and M. ICHIKAWA, 1976, *Abstract for Ann. Meet. Seismol. Soc. Japan*, (in Japanese).
- WATANABE, H., 1974, Determination of earthquake magnitude at regional distance in and near Japan (third report)—On relation between magnitude and period corresponding to the maximum trace amplitude—, *Zisin*, II, **27**, 129-140, (in Japanese).
- WYSS, M., and J. N. BRUNE, 1967, The Alaska earthquake of 28 March 1964: A complex multiple rupture, *Bull. Seism. Soc. Am.*, **57**, 1017-1023.

24. 前震のスペクトル的特徴

地震研究所 辻 浦 賢

大地震に前震を伴う場合がある。若しある地域に発生した地震が、大地震のための前震か、定常活動としての地震であるかを識別出来れば、地震予知のための1つの重要な手がかりとなる。

今回1976年6月に発生した山梨県東部地震 (M 5.5)、同年8月の伊豆、河津地震 (M 5.4) 及び1975年11月のハワイ地震 (M 7.1) の前震本震余震系列、並びに一部定常活動における地震について地震波スペクトルの立場から調べてみた。

今回の結果から前震のスペクトルは本震、或は余震に比べ異なるが、傾向は一樣でなく、例えば応力降下についてみると、山梨、河津両地震の前震はその本震、或は余震に比べ約1/5程度である。一方ハワイ地震の場合は逆に高い。今後スペクトルの帯域巾を拡げ (0.1~200 Hz)、特に近地震スペクトルの時間的経過を追ってゆく予定である。